Angelika Eberhardt*
Dušan Bošković
Stefan Loebbecke
Slobodan Panić
Yannik Winter

Customized Design of Scalable Microfluidic Droplet Generators Using Step-Emulsification Methods

Customized monodisperse microparticles and microcapsules can be produced by combining microfluidic droplet generation with subsequent particle solidification. Established microfluidic devices for droplet formation like flow-focusing structures or T-junctions provide high reproducibility and controllability, but are often limited in terms of throughput or variability. A higher throughput by means of simple numbering-up can be achieved by applying alternative droplet formation mechanisms like step emulsification. Using laser-ablated glass reactors designed in-house, comprehensive studies with varied step geometry and process parameters were performed in order to provide fundamental data for general calculation methods allowing the fast design of customized microfluidic droplet generators.

Keywords: Customized microreactor design, Microfluidic droplet generation, Scale-up, Step emulsification

Received: February 27, 2019; *revised:* May 27, 2019; *accepted:* July 09, 2019

DOI: 10.1002/ceat.201900143

1 Introduction

The industrial application of microparticles and microcapsules with high monodispersity and consistent quality offers a number of specific advantages like simple and controllable dosage or a uniform and dust-free application on large-area materials. Microcapsules have further applications such as the defined release of technical or pharmaceutical agents. Therefore, they serve both as a processing aid and as an end product. Compared to large-scale processes for microparticle production such as spray drying, microstructured devices allow better control of particle size, shape, and morphology by separating the production process into two steps consisting of microfluidic droplet generation and subsequent particle solidification [1].

Using well-known microfluidic devices like flow-focusing structures or T-junctions, droplets with tailored size, shape, and morphology can be produced with a high monodispersity and reproducibility. However, since the droplet breakup mechanism of these techniques is mainly controlled by hydrodynamic forces, scaling-up often leads to a loss of quality or to an increased structural or peripheral complexity which still limits further industrial application. Therefore, recent studies have focused on capacity enhancement while maintaining constant particle quality, e.g., by applying alternative droplet formation mechanisms like step emulsification.

In microfluidic droplet generators with step geometry, the dispersed phase is fed into a second immiscible fluid (continuous phase) through nozzles with significant cross section enlargements, the so-called steps (Fig. 1 a).

Due to the significant change in channel height (size of the step), the droplet breakup is triggered by instabilities occurring along the surface or curvature of the forming droplets, caused by capillary pressure jumps between the immiscible phases [2]. Due to this physical effect, the droplet breakup itself is almost insensitive to the fluid properties, especially to the surface tension [3]. The resulting droplet size, however, is influenced by dynamical effects depending on fluid properties like surface tension and viscosity and the flow rate of the dispersed phase. On the other hand, the impact of the dynamic forces on the droplet size can be influenced by the profile and the dimensions of the microchannel of the dispersed phase and the step geometry (Fig. 1 b) [3, 4].

Removal of the droplets from the nozzles can be induced gravitationally due to the different densities of the immiscible phases, forced by the continuous-phase flow, or the droplets are self-propelled due to the spontaneous droplet breakup [2]. As a result, compared to hydrodynamically controlled droplet generation structures like T-junctions, no surplus of the second phase is mandatory for monodisperse droplet formation, which allows high volume fraction emulsions. Furthermore, no significant influence on droplet size or monodispersity caused by fluctuations in flow rates due to start-up or shut-down procedures, production interruptions, or blocked channels can be observed. Because of these advantages and the specific droplet breakup characteristics at steps with optimized profiles, an

Angelika Eberhardt, Dr. Dušan Bošković, Dr. Stefan Loebbecke, Slobodan Panić, Yannik Winter
angelika.eberhardt@ict.fraunhofer.de
Fraunhofer Institute for Chemical Technology (ICT), Joseph-von-Fraunhofer-Strasse 7, 76327 Pfinztal, Germany.

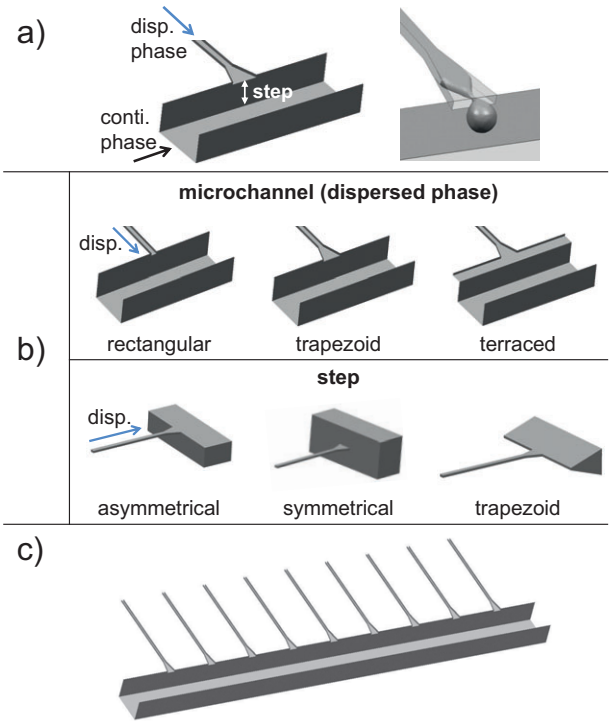

Figure 1. Step emulsification: (a) droplet formation in a step geometry; (b) design variations of microchannel (dispersed phase) and step profile; (c) increase of throughput by numbering-up.

increase in the throughput can easily be achieved by numbering-up steps in a single microfluidic device (Fig. 1 c). Recent publications already proved that increasing the step number up to several hundred does not compromise the monodisperse droplet size distribution [4, 5].

However, the fact that the droplet formation in a step reactor is mainly determined by the device geometry and only weakly depends on physical fluid properties or process parameters also means that variations in product characteristics like droplet size or morphology imply the use of different step reactors. In order to provide suitable step reactors for particular droplet types, reliable relations between droplet formation and step geometry as well as fluid characteristics are mandatory.

In this study, tests with varied microreactor geometry (profile, number, and dimensions of channels and steps), fluid characteristics, and process parameters like volume flow ratio have therefore been performed. These experimental data form the basis for identifying physical principles and dependencies of the droplet formation in step geometries aiming to derive general rules for the fast design and supply of customized microfluidic droplet generators.

2 Experimental

2.1 Step Reactor Design and Fabrication

To study the influence of reactor geometry, fluid characteristics, and process parameters on droplet size and throughput, a set of borosilicate glass microreactors with different geometry and varied numbers of steps were designed and fabricated in-house using laser ablation techniques. Fig. 2 presents a selection of these microreactors outlining the studied parameters.

Fig. 2 a displays a step reactor with 20 steps and two inlet channels for the dispersed and the continuous phase, respectively. The dispersed phase is pumped into the middle channel and injected into the outer continuous-phase channel via two sets of shallow microchannels arranged symmetrically on each side of the middle channel. Fig. 2 b depicts a different microreactor type where the steps are positioned directly on the edge of the glass chip. If the chip is placed in a vessel containing the continuous phase, reduced droplet coalescence tendencies are to be expected because there is no confinement of the newly generated droplets in a constricted channel [6].

For deliberately changing the droplet size, microreactors with varied microchannel (dispersed phase) and step profiles were fabricated. Further increase of throughput was achieved by implementing higher step numbers (Figs. 2 b, 2 c). The laser ablation technique enables the manufacturing of scaled-up step reactors with high accuracy (e.g., MR_300: variation coefficient of the dispersed phase microchannel width of ± 3 µm or 1.6 %, respectively). Tab. 1 lists the step numbers and the geometrical dimensions of the different microreactors. Most of the microreactors were designed with uniform step profiles, except for MR_1.13: here, five different step geometries were positioned in one reactor chip.

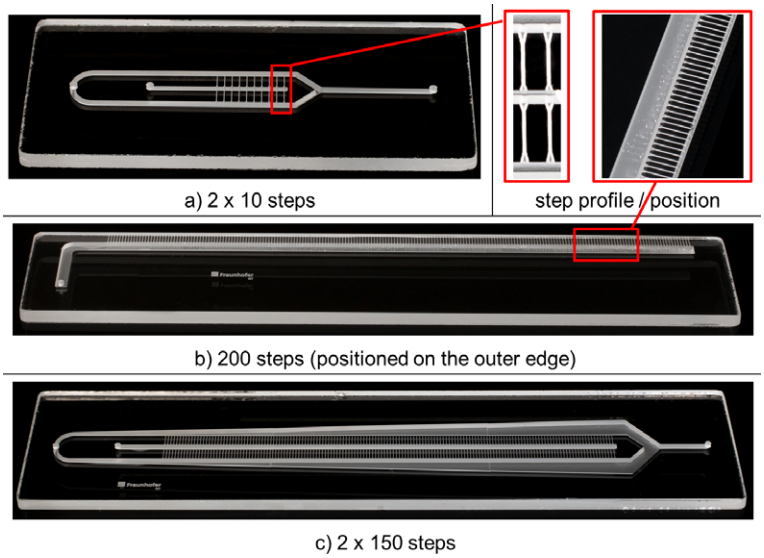

Figure 2. Borosilicate glass microreactor design variations: (a) step reactor with 2×10 steps leading into two symmetrically arranged outer channels; (b) step reactor with 200 steps positioned on the edge of the glass chip; (c) step reactor with 2×150 steps (symmetrical arrangement).

Table 1. Variation of step profile and number of steps. The microreactors MR_1.11–1.14 were designed with uniform dimensions of the inlet channels for the dispersed and the continuous phase. Mean channel top width × bottom width × height: 560 × 170 × 590 µm / 800 × 420 × 590 µm.

Step reactor	Step number	Microchannel/step profile L2 × W2 × H2 [µm]		
MR_1.11	2 × 10	327 × 280 × 90	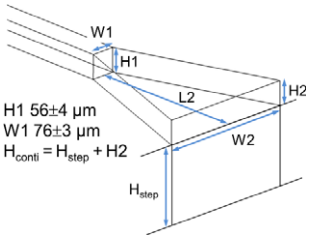	
MR_1.14	2 × 19	322 × 284 × 68		
Varied step height (H2)				
MR_1.12-30 [a), b)]	2 × 10	312 × 180 × 30		
MR_1.12-75	2 × 10	312 × 180 × 76		
MR_1.12-100 [b), c)]	2 × 10	312 × 180 × 104		
Multimodal emulsions			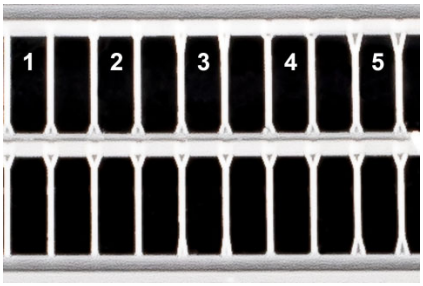	
MR_1.13	2 × 10			
Step profile 1	2 × 2	NA × 78 × 58		
Step profile 2	2 × 2	123 × 175 × 84		
Step profile 3	2 × 2	500 × 191 × 88		
Step profile 4	2 × 2	123 × 278 × 86		
Step profile 5	2 × 2	528 × 290 × 84		
Numbering-up			Inlet channel (disp. phase)	Inlet channel (conti. phase)
			$B \times H$ [µm]	
MR_200	200	H2 = 76 ± 5	2000 × 700	–
MR_300	2 × 150	312 × 180 × 79 ± 3	750 × 750	750-4000 × 750

[a)] H1 = 30 µm; [b)] inlet channel disp./conti. phase: height 850 µm; [c)] H1 = 94 µm.

In order to prevent polydisperse or unstable droplet generation, the channel dimensions and the flow rate distribution within the microfluidic devices were optimized by performing computational fluid dynamics (CFD) calculations using the simulation software package ACE+ Suite (Advanced CFD & Multiphysics, ESI). As an example, Fig. 3 illustrates the optimization of a microreactor with 2×10 steps. By varying the height and width of the inlet channel of the dispersed phase, and particularly the length and the cross-sectional area of the microchannels leading to the steps, an equal pressure distribution in all of the microchannels was achieved, resulting in a uniform flow rate at each individual step.

2.2 Materials and Methods

The influence of fluid characteristics like the dynamic viscosity of the dispersed phase was examined with three different

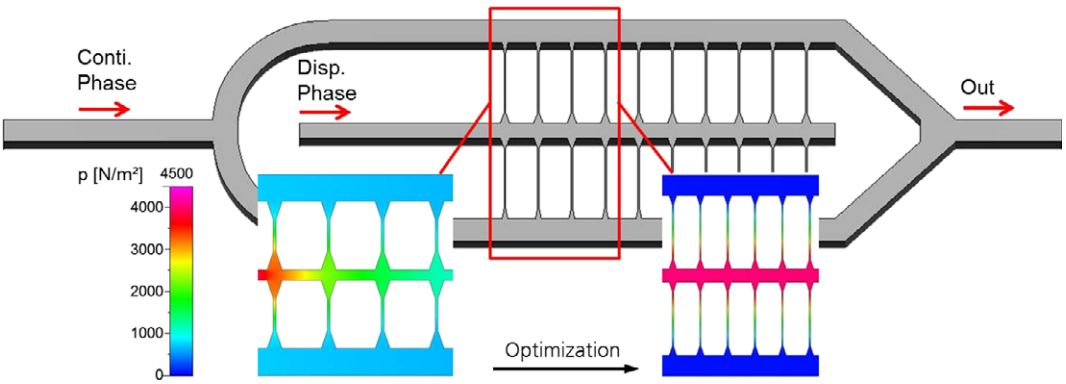

Figure 3. Optimization of flow rate distribution by means of CFD calculations with varied microchannel (dispersed phase) and step dimensions.

organic liquids (Tab. 2). The continuous phase was prepared by mixing deionized water with 0.3 % anionic surfactant, i.e., sodium dodecyl sulfate (SDS; Alfa Aesar, 99 %).

Table 2. Fluid characteristics of organic liquids used as dispersed phase.

Liquids	Dynamic viscosity [mPa s]	Density [g cm^{-3}]	Supplier
Trichloromethane	0.56	1.49	Fluka ≥ 99.8 %
n-Decane	0.92	0.73	Merck > 99 %
Paraffin oil (low viscosity)	40–50	0.84–0.85	Carl Roth

Syringe pumps (neMESYS, Cetoni) were used to inject the dispersed and the continuous phase into the step reactor. The droplet generation frequency as well as the droplet size and stability immediately after droplet breakup were determined by mounting the step reactors on the stage of an inverted light microscope (Leica DMI5000 M) and recording videos with a high-speed camera (Phantom Miro 340). Offline determination of the droplet size and the coalescence behavior during storage was performed by visual analysis using the Java-based image processing program ImageJ (1.48v).

3 Results and Discussion

3.1 Droplet Generation with Varied Process Parameters and Fluid Properties

Droplet formation experiments with varied volume flow rates of the dispersed (Q_{disp}) and the continuous phase (Q_{conti}) in the range of 1–250 µL min^{-1} were performed using three different organic liquids as dispersed phase (trichloromethane, *n*-decane, paraffin oil; Tab. 2). Depending on the dynamic viscosity of the dispersed phase monodisperse droplets with a maximum variation coefficient CV of 4.4 % could be produced over a wide range of flow rates.

Fig. 4 shows an example of the production of trichloromethane droplets with a step reactor with 2×10 steps. For all three organic liquids a minimum dispersed flow rate (1 µL min^{-1} per step for trichloromethane and *n*-decane, 0.5 µL min^{-1} per step for paraffin oil) was needed to ensure stable droplet formation at all steps. While in the studied dispersed flow rate range no maximum flow rate was detectable for the low viscosity organic liquids (maximum flow rate tested: 12.5 µL min^{-1} per step), paraffin oil droplets were only producible up to 2 µL min^{-1} per step, demonstrating the strong influence of the viscosity of the dispersed phase on the operational range. The use of higher dispersed flow rates led to unstable and polydisperse droplet formation.

Within the operational range of both flow rates, long-term test series proved the stability of the droplet formation, e.g., a variation coefficient CV of 0.7 % within a 7-h run of producing trichloromethane droplets in deionized water with 0.3 % SDS

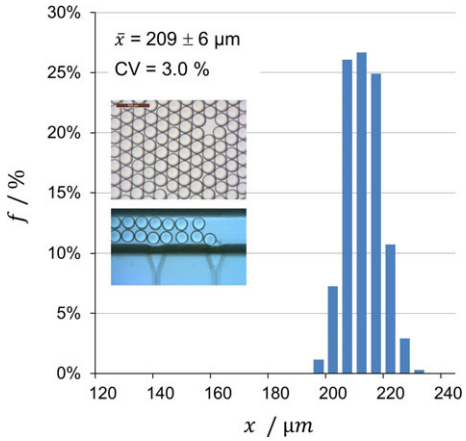

Figure 4. Droplet size distribution of trichloromethane droplets in deionized water with 0.3 % SDS. Q_{disp}/Q_{conti} = 50/200 µL min^{-1}, step reactor MR_1.12–75.

(mean droplet size 207 ± 1.5 µm; Q_{disp}/Q_{conti} = 40/100 µL/min; MR_1.12–75 µm).

Tests with trichloromethane and two different step reactor geometries confirmed the dependency of the droplet size on the step size, while revealing no significant influence of the continuous-phase flow rate (Fig. 5). Further experiments with *n*-decane and paraffin oil using the presented step reactors with optimized trapezoid profiles of the dispersed-phase channel proved that dynamic effects like fluid characteristics and dispersed-phase flow have a limited influence.

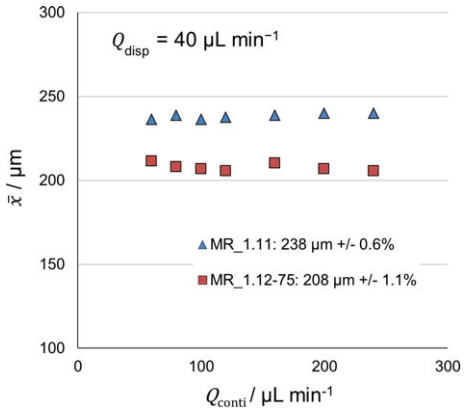

Figure 5. Effect of continuous-phase flow rate Q_{conti} and step geometry on the mean droplet size $\bar{x}$. Dispersed phase: trichloromethane, constant flow rate Q_{disp} 40 µL min^{-1}; varied microchannel width and height (MR_1.11: 280×90 µm, MR_1.12–75: 180×76 µm).

While the droplet size of all three organic liquids used as dispersed phase slightly increased linearly with growing dispersed-flow rate, there was no significant influence of the fluid characteristics (Fig. 6). Even though the results did not reveal a significant influence of the continuous phase on the droplet size, further expansion of the flow rate range showed that depending on the dispersed-phase flow rate minimum and max-

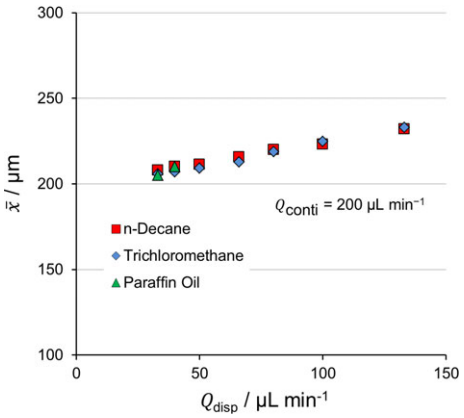

Figure 6. Effect of fluid characteristics and flow rate of dispersed phase Q_{disp} on the mean droplet size $\bar{x}$. Continuous phase: 0.3 % SDS in deionized water, constant flow rate Q_{conti} = 200 µL min^{-1}; step reactor: MR_1.12–75.

imum continuous-phase flow rates were needed for a stable droplet formation. Continuous-phase flow rates below a minimum value of 1.5×Q_{disp} led to insufficient droplet transportation with progressive droplet coalescence in the continuous-flow outlet channels, whereas continuous-phase flow rates exceeding maximum values of 10×Q_{disp} resulted in unequal distribution of the dispersed phase and blocking of individual microchannels.

3.2 Effect of Step Geometry

Three different step reactors were used to study the influence of the step geometry. Increasing the height of the microchannel opening into the step led to an approximately linear increase of the mean droplet size with equivalently reduced droplet generation frequencies f while maintaining the narrow droplet size distribution (Figs. 7 a, 7 b).

The stable droplet generation combined with the strong relation between step geometry and droplet size enables the production of droplets with controlled multimodal size distributions in one single microreactor chip, e.g., bi- or trimodal droplet ensembles. Fig. 8 presents experimental results of a step reactor containing five different step profiles (MR_1.13, Tab. 1) which was employed to produce droplets with a multimodal size distribution. Because of the minor influence of the continuous-phase flow, at each different step structure droplets with varying droplet sizes were generated, thus forming a mixture containing five different mean droplet sizes (Fig. 8 d).

3.3 Numbering-up

Increasing the step number up to 300 steps, a maximum throughput of 4000 µL min^{-1} (13.3 µL min^{-1} per step) of dispersed phase was achievable (trichloromethane in deionized water with 0.3 % SDS, Fig. 9 a), only limited by the confinement within the continuous-phase channel. Experiments with step reactors with a larger cross section of the continuous-phase channel proved that the use of larger outlet channel dimensions

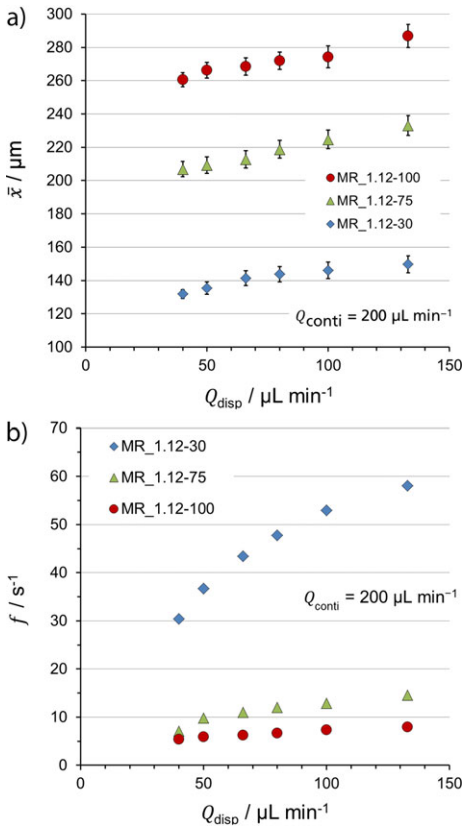

Figure 7. Effect of step geometry and dispersed-phase flow rate on (a) mean droplet size $\bar{x}$ and (b) droplet frequency f per step. Dispersed phase: trichloromethane in deionized water with 0.3 % SDS; varied microchannel height: 30/76/104 µm, constant width: 180 µm.

enables further throughput enhancement without the risk of droplet coalescence. Despite the high number of produced droplets no impact on droplet breakup or monodispersity could be observed, provided that the continuous-phase flow rate was at least as high as the dispersed flow rate ($Q_{conti} \geq Q_{disp}$).

Comparative tests with two step reactors containing 20 and 300 steps and a comparable step profile (MR_1.12-75/MR_1.12-300D) produced droplets with similar mean droplet sizes while maintaining the same narrow droplet size distribution (Fig. 9 b). The actual droplet size difference can be attributed to manufacturing tolerances due to optical effects of the laser ablation technique causing slightly higher step dimensions within the scaled-up microreactor. This confirms the assumption that the droplet size and monodispersity are mainly determined by the step profile as long as the removal of the droplets after breakup is provided.

Restrictions caused by insufficient removal of the droplets due to limited continuous-flow rate or constricted channel dimensions can be alleviated by positioning the steps on the edge of the glass chip (Fig. 2 b). Emulsions are produced by placing the step reactor in a vessel containing the continuous phase. While no influence of position or orientation of the device on productivity or droplet size uniformity has been

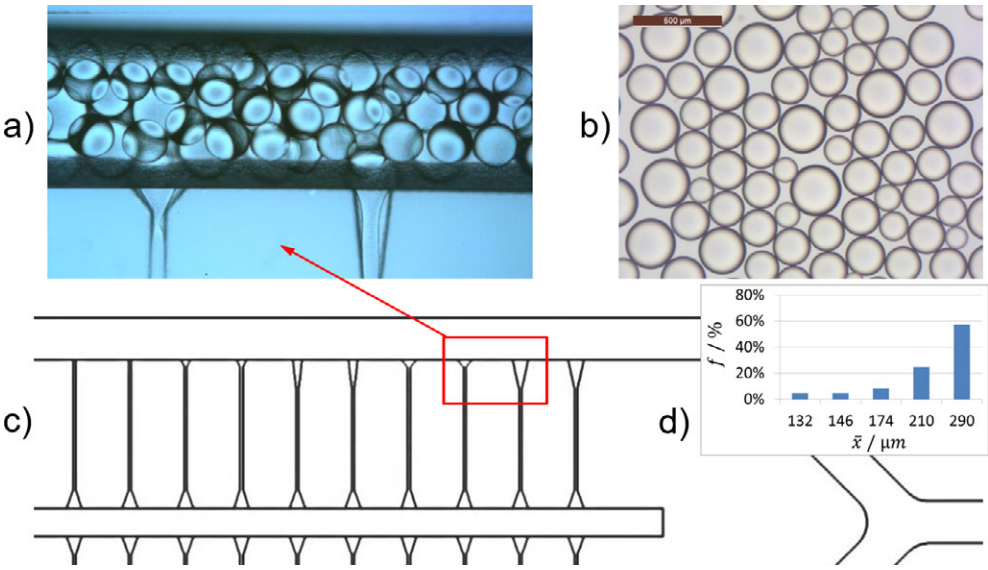

Figure 8. Controlled droplet production with multimodal droplet size distribution (trichloromethane in deionized water with 0.3 % SDS, Q_{disp}/Q_{conti} = 60/120 µL min^{-1}): (a) droplet formation at two different steps; (b) multimodal droplets; (c) sketch of the step reactor with five different step profiles (MR_1.13, Tab. 1); (d) droplet size distribution with five different mean droplet sizes.

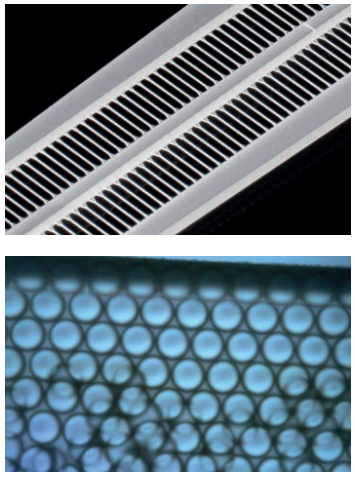

	MR_1.12-75	MR_1.12-300D
Step number	20	300
Q_{disp} [µL min^{-1}]	66	1000
per step	3.3	3.3
Mean droplet size [µm]	213±6	243±4

a) b)

Figure 9. Numbering-up: (a) production of trichloromethane droplets in a step reactor with 300 steps (Q_{disp}/Q_{conti} = 1000/2000 µL min^{-1}, 0.3 % SDS in deionized water); (b) comparison of mean droplet size in step reactors with different step number but comparable step profile.

observed using step reactors with closed continuous-phase channels, further experiments are needed in order to examine the effect of orientation using reactors with lateral steps.

Because of the step characteristics, no stirring or pumping of the continuous phase is needed in order to produce emulsions with narrow droplet size distributions and controlled droplet sizes. Furthermore, significantly reduced droplet coalescence after breakup is observed. This reactor type is therefore particularly suited for emulsions with a high coalescence tendency like polymer solutions used for particle production via solvent evaporation. Fig. 10 presents an example of the production of polystyrene particles with said step reactor. Both droplets and dried particles show a high monodispersity.

4 Conclusions

Using laser-ablated borosilicate glass step reactors with varied geometry and number of steps, stable droplet formation with high monodispersity could be achieved over a wide range of flow rates and flow rate ratios. A comparison of different step designs revealed a significant correlation between step profile/dimensions and droplet size. In contrast, no significant impact of fluid viscosity (dispersed phase), step number, or continuous-flow rate on the mean droplet size could be observed, which enables droplets to be produced with consistent droplet size and monodispersity even after increasing the throughput by several orders of magnitude or by changing the fluid characteristics of the dispersed phase, e.g., through different formulations.

Limitations due to insufficient droplet removal which may lead to increased coalescence or even blocking of individual step structures can be efficiently alleviated by preventing constricted continuous-phase channels or by placing the steps on the edge of the reactor. By positioning different step structures in one single microreactor, tailored multimodal droplet distributions can be produced, because the mass fraction and droplet size of the different droplet portions are adjustable by the geometry and the number of the particular step structures.

In order to predict the step profile needed for a given product (droplet size, fluid characteristics, and throughput), further experiments examining the influence of microreactor geometry and fluid or material characteristics are needed to provide sufficient data for setting up general calculation methods for the fast design of customized scaled-up droplet generators.

The authors have declared no conflict of interest.

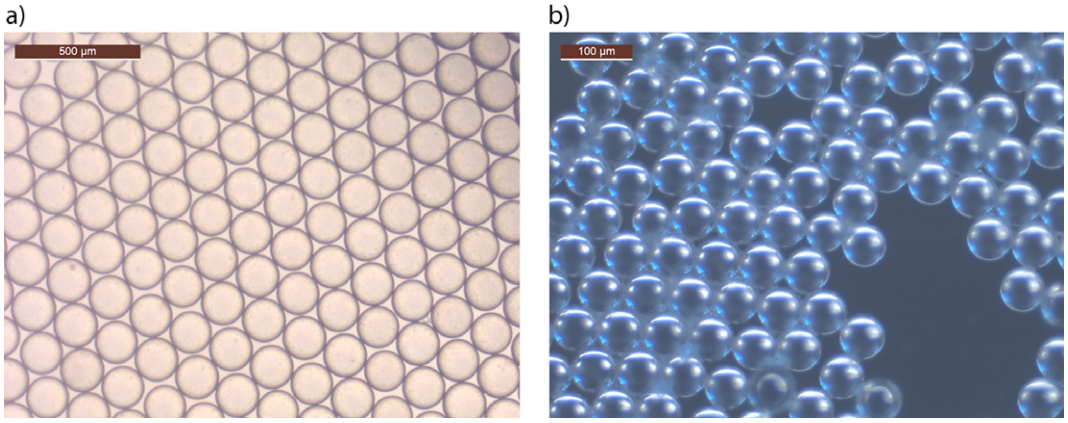

Figure 10. Production of polystyrene (PS) particles (reactor with 200 steps on the edge of the chip, MR_200): (a) droplet formation with a solution of 5 wt % polystyrene in trichloromethane (Q_{disp} = 50 µL min^{-1}); continuous phase: 0.3 wt % SDS in deionized water (0 µL min^{-1}); mean droplet size: 170 ± 2.7 µm; (b) resulting particles after solvent evaporation at 40 °C (24 h), mean particle size 59 ± 1.6 µm.

Symbols used

f	[s^{-1}]	droplet formation frequency
Q_{conti}	[m^{3}s^{-1}]	volume flow rate of continuous phase
Q_{disp}	[m^{3}s^{-1}]	volume flow rate of dispersed phase
x	[m]	droplet size
$\bar{x}$	[m]	mean droplet size

Abbreviations

CFD	computational fluid dynamics
conti	continuous phase
CV	variation coefficient
disp	dispersed phase
SDS	sodium dodecyl sulfate

References

[1] J. Wang et al., *Micromachines* **2017**, *8 (1)*, 22. DOI: https://doi.org/10.3390/Mi8010022
[2] R. Dangla, S. C. Kayi, C. N. Baroud, *Proc. Natl. Acad. Sci. U. S. A.* **2013**, *110 (3)*, 853–858. DOI: https://doi.org/10.1073/pnas.1209186110
[3] R. Dangla, E. Fradet, Y. Lopez, C. N. Baroud, *J. Phys. D: Appl. Phys.* **2013**, *46*, 114003. DOI: https://doi.org/10.1088/0022-3727/46/11/114003
[4] E. Amstad et al., *Lab Chip* **2016**, *16 (21)*, 4163–4172. DOI: https://doi.org/10.1039/c6lc01075j
[5] A. Ofner et al., *Macromol. Chem. Phys.* **2017**, *218 (2)*, 1600472. DOI: https://doi.org/10.1002/macp.201600472
[6] E. Stolovicki, R. Ziblat, D. A. Weitz, *Lab Chip* **2018**, *18 (1)*, 132–138. DOI: https://doi.org/10.1039/c7lc01037k

